Characterization of external refractive index sensitivity of a photonic crystal fiber long-period grating

Fei Tian[1,*], Jiri Kanka[2], and Henry Du[1]

[1]*Department of Chemical Engineering and Materials Science, Stevens Institute of Technology, Hoboken, NJ 07030, USA*

[2]*Institute of Photonics and Electronics AS CR, v.v.i., Chaberska 57, Prague 8, 18251 Czech Republic*

**Corresponding author: ftian1@stevens.edu*

Received April 4, 2015; accepted May 7, 2015; posted online June 1, 2015

Long-period gratings (LPGs) are fabricated in a photonic crystal fiber (PCF) using the symmetric point-by-point CO_2 laser irradiation method to explore the sensitivity characterization of PCF–LPG. Numerical simulation is used to guide the investigation. It is found that the refractive index (RI) sensitivity of PCF–LPG depends on the coupled cladding modes as well as the coupled resonance wavelength (RW) of the LPG. Experimental studies show that the longer the RW, the higher the RI sensitivity for the same cladding mode. At similar RWs, the lower the cladding mode, the higher the RI sensitivity of PCF–LPG.

OCIS codes: 050.0050, 060.2370, 050.5298.

doi: 10.3788/COL201513.070501.

Optical fiber-based sensors have been extensively studied due to the advantages over traditional sensors, including immunity to the electromagnetic field, compatibility for system integration, fast speed, and efficient cost[1]. It has a variety of applications ranging from gas, chemical, to biological sensing[2–8]. Conventional all-solid single-mode fiber-based index sensor presents itself as a great advantage for monitoring the resonance wavelength (RW), but they are subject to a temperature effect which requires an additional compensation sensing scheme[9]. Photonic crystal fibers (PCFs) are a specialty micro-structured optical fiber, with cladding composed of an array of air channels running along the fiber axis. The freedom in designing the micro-structure of the cladding of PCF and the ability to tailor the structure according to specific needs greatly expanded the application of PCF in sensing applications in recent years. Long-period grating (LPG) couples the light from the fundamental core mode to the co-propagating cladding modes, expanding the evanescent field throughout the entire cladding air channels of the PCF. Even better, Petrovic *et al.* found that a PCF–LPG is sensitive to the strain and surrounding refractive index (RI) with very weak response to temperature[10], which greatly reduced the aforementioned issues related to cross sensitivity of a conventional fiber with a doped core. PCF–LPG is thus a flexible platform for optical sensing for a wide range of analytes with a variety of configurations. PCF–LPG-based sensing schemes have been increasingly explored in recently years[11–19]. For example, a PCF–LPG with a RI sensitivity of about 10^{-4} has been demonstrated to measure the thickness of DNA, which is mobilized in the surface of the air channels as a monolayer[20]. While the PCF–LPG is very attractive as a RI transduction platform for sensing applications, the investigation into the sensitivity characterization with respect to the coupled cladding mode and the RW has been limited.

For conventional opticals fiber containing a doped core to have an increased RI, fabrication of LPG is usually through UV irradiation. For PCF made of pure silica, the core of the fiber is no longer sensitive to UV irradiation, such that non-UV methods are generally preferred for the LPG fabrication in PCF. There fabrication techniques include CO_2 laser[21], electric arc,[22] or mechanical microdeformation[23].

We report the study of the sensitivity dependence of PCF–LPG on the coupled cladding mode and the RW. Symmetric CO_2 irradiation method aided by a pair of 120° angled mirrors is used for the fabrication of PCF–LPG to have a symmetric mode-coupling[21]. A mode solver based on the finite-element method (FEM) is used to calculate the phase matching curves for the cladding mode of $LP_{0,2}$, $LP_{0,3}$, and $LP_{0,4}$. PCF–LPGs coupled with different cladding modes and RWs are fabricated using the symmetric CO_2 laser irradiation method. RI measurement is done by using a glycerin–water mixture as a means to change the surrounding RI of the PCF–LPG. It is revealed that for the PCF–LPGs coupled with the same cladding mode, the longer the RW, the higher the sensitivity. For PCF–LPGs coupled at similar RWs, the lower the cladding mode, the higher the sensitivity.

The PCF used in this work is endlessly single-mode fiber ESM-12B from NKT Photonics. It has a solid core and six rings of air channels in the cladding with a hole diameter of ~3.2 μm and pitch of ~8 μm as shown by the scanning electron microscopy (SEM) image in the inset of Fig. 1. We first attempted theoretical simulation to study the mode orders with respect to the periodicity of perturbation. A mode solver (COMSOL Multiphysics, extended with the radio frequency module) based on the FEM was employed to calculate the phase matching conditions for different cladding modes and the field profiles. The geometric profile extracted from the SEM image of the

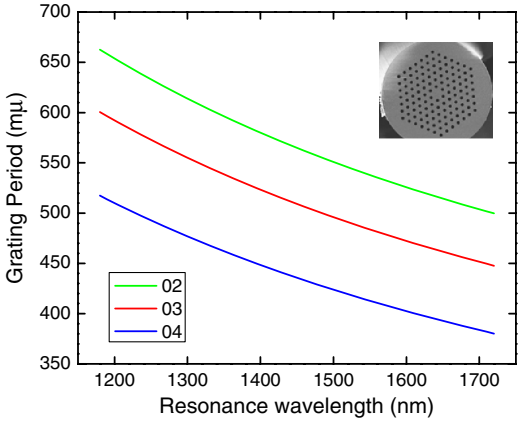

Fig. 1. Phase matching curves of the $LP_{0,n}$ cladding modes. Inset, SEM image of the cross sectional area of ESM-12B.

PCF is used as the input for the numerical calculation. For symmetric perturbation, only the symmetric $LP_{0,n}$ cladding modes are coupled and considered in this work. The resonance condition for mode coupling is governed by the phase matching condition $\lambda_i = (n_{core}^{eff,} - n_{clad(i)}^{eff,})\Lambda$, where λ_i is the RW of the ith cladding mode, and $n_{core}^{eff,}$ and $n_{clad(i)}^{eff,}$ are the effective refractive indices of the fundamental core mode and the ith cladding mode, respectively. Figure 1 shows the phase matching curves for the $LP_{0,2}$, $LP_{0,3}$, and $LP_{0,4}$ modes. It shows that for all the three cladding modes considered in this work, the longer the RW, the shorter the periodicity.

PCF–LPGs are fabricated using the CO_2 laser system described elsewhere[24] with a set of pre-selected periodicities in order to couple $LP_{0,4}$ cladding mode at different RWs. The periodicities are 380, 410, and 490 μm with the corresponding coupled RWs at 1697.2, 1585.6, and 1291.6 nm, respectively. The periodicities and their corresponding RWs are generally in agreement with the phase-matching curve of $LP_{0,4}$ mode in Fig. 1.

The transmission spectra of the as-fabricated PCF–LPG coupled with $LP_{0,4}$ cladding mode at different RWs are shown in Fig. 2. Note that the experimental RWs are not exactly the same as the values calculated in the simulation at the same grating periodicities. It is possible that the fluctuations in the CO_2 laser power output during the fabrication contribute to the slight deviation.

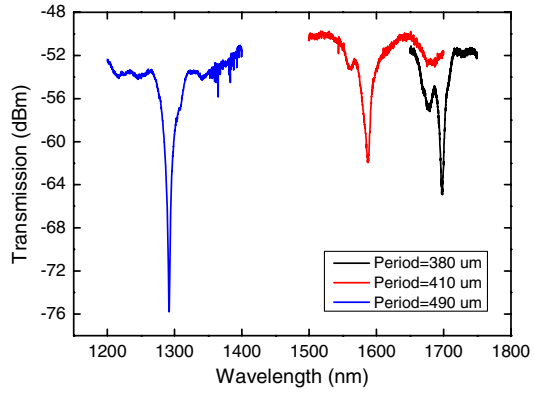

Fig. 2. Transmission spectra of PCF–LPG coupled with $LP_{0,4}$ mode fabricated with periodicities of 380, 410, and 490 μm.

The variations of the RI of the surrounding medium influence the λ_i of the LPG, which can be described by the following[25]

$$\frac{\partial \lambda_i}{\partial n_{sur}} = \left[\frac{\partial n_{core}^{eff}(\lambda_i, n_{sur})}{\partial n_{sur}} - \frac{\partial n_{clad(i)}^{eff}(\lambda_i, n_{sur})}{\partial n_{sur}}\right]\Lambda, \quad (1)$$

where n_{sur} is the RI of the surrounding medium and $n_{core}^{eff,}(\lambda_i, n_{sur})$ and $n_{clad(i)}^{eff,}(\lambda_i, n_{sur})$ are the effective indices of the fundamental core mode and the ith cladding mode, respectively. The term $\partial n_{clad(i)}^{eff}(\lambda_i, n_{sur})/\partial n_{sur}$ is correlated to each cladding mode, such that the spectral response of LPG depends strongly on the order of the coupled cladding mode. To evaluate the response of the PCF–LPG to the RI in the surrounding medium, we immerse the PCF–LPG in a glycerin–water mixture with concentration ranging from 0% to 40% as a means to change the surrounding RI. At 1550 nm and room temperature, pure water and glycerin have RIs of 1.318 and 1.462[26], respectively. Light from a SuperK supercontinuum light source is launched through the fiber.

An optical spectrum analyzer (OSA) with a resolution of 0.05 nm was used to measure the transmission spectra of the PCF–LPGs during the measurements. A number of PCF–LPGs are tested under the same conditions. Shown in Fig. 3 are the transmission spectra and response of the three PCF–LPGs for the RWs shift with respect to the change in the RI of the surrounding medium.

It is seen from Fig. 3 that when the surrounding RI increases, there is a red shift in the RWs of all the three

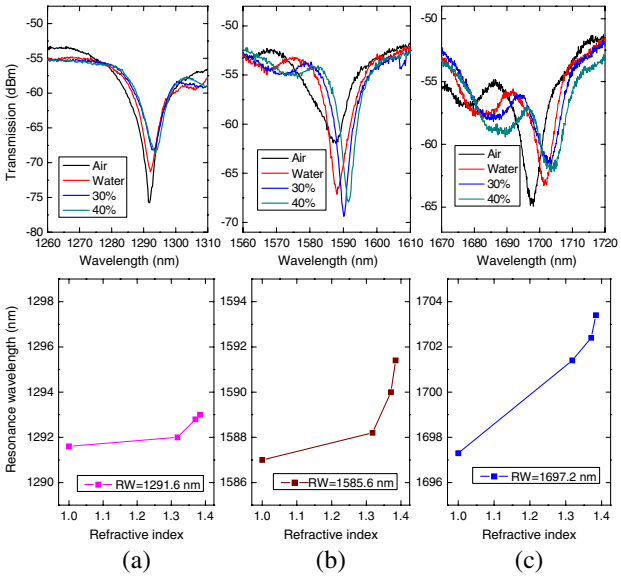

Fig. 3. Transmission spectra (top) and response (bottom) of PCF-LPG to the change of surrounding RI for $LP_{0,4}$ cladding mode with RW of the following: (a) 1291.6, (b) 1585.6, and (c) 1697.2 nm.

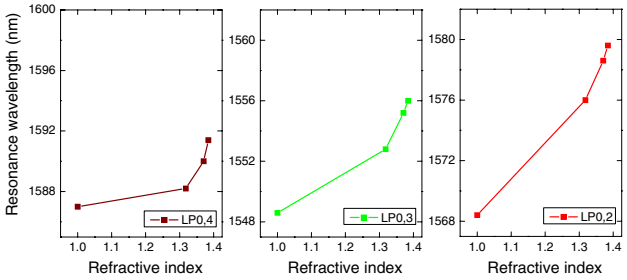

Fig. 4. Dependence of RW on the surrounding RI of PCF–LPGs coupled with $LP_{0,2}$, $LP_{0,3}$, and $LP_{0,4}$ cladding modes.

LPGs investigated. This is because when the surrounding RI increases, the changes in the effective indices of the core mode and cladding mode are dominated by the dispersion such that $\partial n_{core}^{eff}(\lambda_i, n_{sur})/\partial n_{sur} > \partial n_{clad(i)}^{eff}(\lambda_i, n_{sur})/\partial n_{sur}$. Obviously the response of LPG with RW of 1697.2 nm is greater than that of the LPG with RW 1585.6 nm. The response of LPG with RW of 1585.6 nm is greater than that of the LPG with RW of 1291.6 nm. This is due to the fact that evanescent overlap at the longer wavelength is greater than that at shorter wavelength. It is noticed that there is more noise in the longer wavelength than in the shorter wavelength. A possible reason is that the light source we use has more noise at a longer wavelength.

In order to examine the dependence of the RI sensitivity to the order of the coupled cladding modes, PCF–LPG coupled with $LP_{0,2}$, $LP_{0,3}$, and $LP_{0,4}$ cladding modes are fabricated at the RWs around 1550 nm with the periodicities of 550, 475, and 410 μm, respectively. The as-fabricated PCF–LPGs are with $LP_{0,2}$, $LP_{0,3}$, and $LP_{0,4}$ cladding modes coupled at 1568, 1549.2, and 1585.6 nm, respectively. The resultant PCF–LPGs are immersed in the same glycerin–water mixture with concentration ranging from 0% to 40% to evaluate their RI sensitivities. Figure 4 shows the RWs shift for the PCF–LPGs coupled with $LP_{0,2}$, $LP_{0,3}$, and $LP_{0,4}$ cladding modes as the RI of the surrounding medium changes.

Figure 4 shows that while there is always red shift in the RW as the surrounding RI increases for all the three cladding modes considered, the sensitivities are different. The $LP_{0,2}$ mode has the highest RI sensitivity among the three PCF–LPGs examined in this work. The RI sensitivity of PCF–LPG increases with the decrease of the order of the cladding mode coupled. The lower the cladding mode, the higher the RI sensitivity.

In conclusion, we investigate the RI sensitivity of PCF–LPG with respect to the RW and coupled cladding modes. We show that for a PCF–LPG coupled with a distinct cladding mode, the longer the RW, the higher the sensitivity. The lower the coupled cladding mode, the higher the RI sensitivity. The sensitivity can be further improved by careful design of the microstructure of the PCF and LPG fabrication. This work can be used to guide the design and fabrication for PCF–LPG as a powerful alternative for chemical and biological sensing applications.

This work was supported by the United States National Science Foundation under Grant No. DMR-1206669 and by the Ministry of Education, Youth, and Sport of the Czech Republic under Grant No. LH 11038 within the U.S.–Czech S&T Cooperation agreement.

References

1. B. Lee, Opt. Fiber Technol. **9**, 57 (2003).
2. F. Tian, J. Kanka, X. Li, and H. Du, Proc. SPIE **9098**, 90980R (2014).
3. H. Chen, F. Tian, J. Chi, and H. Du, Proc. SPIE **9098**, 90980T (2014).
4. N. Wang, Y. Zhu, T. Gong, L. Li, and W. Chen, Chin. Opt. Lett. **11**, 070601 (2013).
5. H. Chen, F. Tian, J. Kanka, and H. Du, Appl. Phys. Lett. **106**, 111102 (2015).
6. W.-H. Tsai, K.-C. Lin, S.-M. Yang, Y.-C. Tsao, and P.-J. Ho, Chin. Opt. Lett. **12**, 042801 (2014).
7. P. Jia and D. Wang, Chin. Opt. Lett. **11**, 040601 (2013).
8. H. Chen, F. Tian, J. Chi, J. Kanka, and H. Du, Opt. Lett. **39**, 5822 (2014).
9. X. Yu, P. Shum, G. B. Ren, and Y. Zhang, in *2008 IEEE Photonics Global at Singapore, IPGC*, paper 4781448 (2008).
10. J. S. Petrovic, H. Dobb, V. K. Mezentsev, K. Kalli, D. J. Webb, and I. Bennion, J. Lightw. Technol. **25**, 1306 (2007).
11. L. Rindorf and O. Bang, J. Opt. Soc. Am. B **25**, 310 (2008).
12. F. Tian, J. Kanka, X. Li, and H. Du, Sens. Actuators B **196**, 475 (2014).
13. S. Zheng, Y. Zhu, and S. Krishnaswamy, Sens. Actuators B **176**, 264 (2013).
14. F. Tian, J. Kanka, S. A. Sukhishvili, and H. Du, Opt. Lett. **37**, 4299 (2012).
15. S. Zheng, Struct. Health Monitor. **14**, 148 (2015).
16. F. Tian, J. Kanka, and H. Du, Opt. Express **20**, 20951 (2012).
17. A. Cusano, M. Consales, A. Crescitelli, and A. Ricciardi, *Lab-On-Fiber Technology* (Springer, 2015).
18. F. Tian, Z. He, and H. Du, Opt. Lett. **37**, 380 (2012).
19. Z. He, F. Tian, Y. Zhu, N. Lavlinskaia, and H. Du, Biosens. Bioelectron. **26**, 4774 (2011).
20. L. Rindorf, J. B. Jensen, M. Dufva, L. H. Pedersen, P. E. Høiby, and O. Bang, Opt. Express **14**, 8224 (2006).
21. F. Tian, J. Kanka, B. Zou, K. S. Chiang, and H. Du, Opt. Express **21**, 13208 (2013).
22. G. Humbert, A. Malki, S. Fevrier, P. Roy, and D. Pagnoux, Electron. Lett. **39**, 349 (2003).
23. M. D. Nielsen, G. Vienne, J. R. Folkenberg, and A. Bjarklev, Opt. Lett. **28**, 236 (2003).
24. F. Tian, J. Kanka, B. Zou, K. S. Chiang, and H. Du, Proc. SPIE **8722**, 87220I (2013).
25. Y. Zhu, Z. He, and H. Du, Sens. Actuators B **131**, 265 (2008).
26. J. Hetrick, *Characteristic Sheet of OHGL* (Cargille, 2006).